Espinos A, Romero ML, Serra E, Hospitaler A. Experimental investigation on the fire behaviour of rectangular and elliptical slender concrete-filled tubular columns. Thin-Walled Struct. 2015;93:137-48. doi: 10.1016/j.tws.2015.03.018

Experimental investigation on the fire behaviour of rectangular and elliptical slender concrete-filled tubular columns

A. Espinos [a]*, M. L. Romero [a], E. Serra [a], A. Hospitaler [a]

[a] *Instituto de Ciencia y Tecnología del Hormigón (ICITECH), Universitat Politècnica de València, Valencia, Spain*
* *Corresponding author. e-mail address: aespinos@mes.upv.es*

ABSTRACT

While the fire behaviour of concrete-filled steel tubular (CFST) columns with circular and square cross-section has been well established based on experimental programs and numerical investigations, the information about the fire behaviour of CFST columns with rectangular or elliptical cross-section is very scarce. Therefore, further research is needed in order to establish the structural behaviour of concrete-filled elliptical and rectangular hollow sections at elevated temperatures as a basis for the future development of new design guidance. In this paper, a series of slender CFST columns of rectangular and elliptical cross-section are tested at elevated temperatures under both concentric and eccentric loads, reaching large eccentricities. The effect of the load eccentricity and percentage of reinforcement is studied, considering both major and minor axis buckling. The influence of the cross-section shape, load eccentricity and percentage of reinforcement on the fire behaviour of these columns is investigated. The experimental results are subsequently used to assess the current design rules in Eurocode 4 Part 1.2 for these new section shapes.

Keywords: *Fire resistance; Concrete-filled tubular columns; Large eccentricities; Slender columns; Rectangular hollow sections; Elliptical hollow sections; Eurocode 4; Simple calculation model*

NOTATION

A_i	Cross-sectional area of the of the part *i* of the composite section
B	Smaller outer dimension of an elliptical or rectangular section
B.C.	Boundary conditions
CFST	Concrete-filled steel tube
e	Load eccentricity
$E_{a,\theta}$	Modulus of elasticity of structural steel at the temperature θ
$E_{c,sec,\theta}$	Secant modulus of concrete at the temperature θ
$E_{s,\theta}$	Modulus of elasticity of reinforcing steel at the temperature θ
$(EI)_{fi,eff}$	Effective flexural stiffness in the fire situation
EC4	Eurocode 4
EHS	Elliptical hollow section
f_c	Compressive cylinder strength of concrete at room temperature (test date)
f_s	Yield strength of reinforcing steel at room temperature
f_y	Yield strength of structural steel at room temperature
H	Larger outer dimension of an elliptical or rectangular section
$I_{i,\theta}$	Second moment of area of the part *i* of the cross-section at the temperature θ
ℓ_θ	Buckling length of the column in the fire situation
L	Column length
N	Test load
$N_{fi,cr}$	Elastic critical load in the fire situation
$N_{fi,pl,Rd}$	Design value of the plastic resistance of the cross-section to axial compression in the fire situation
$N_{fi,Rd}$	Design axial buckling load in the fire situation
$N_{fi,Rd,\delta}$	Design axial buckling load in the fire situation in case of eccentric load
N_{Rd}	Design axial buckling load at room temperature
$N_{Rd,\delta}$	Design axial buckling load at room temperature in case of eccentric load
P-P	Pinned-pinned boundary conditions
RHS	Rectangular hollow section
t	Steel tube wall thickness
$\gamma_{M,fi,i}$	Partial factors for the materials in the fire situation
ϕ	Diameter of a reinforcing bar
θ	Temperature
$\bar{\lambda}_y$	Relative slenderness at room temperature, for major axis buckling

$\overline{\lambda}_z$	Relative slenderness at room temperature, for minor axis buckling
$\overline{\lambda}_\theta$	Relative slenderness in the fire situation
ρ	Percentage of reinforcement
$\varphi_{i,\theta}$	Reduction coefficient depending on the effect of thermal stresses
φ_s	Reduction coefficient depending on the percentage of reinforcement
φ_δ	Reduction coefficient depending on the eccentricity
χ	Reduction coefficient for the corresponding buckling curve

1. INTRODUCTION

The use of circular and square hollow sections in composite construction has been widely documented, and the behaviour of such hollow sections filled with concrete has been extensively investigated, both at room temperature and in the fire situation. Many examples of experimental investigations on circular and square CFST columns at elevated temperatures can be cited, as the research projects from CIDECT [1][2][3] and National Research Council of Canada [4][5][6], or the investigations carried out by Han, Zhao and co-workers [7], Kim et al. [8] and the authors of this paper [9][10]. However, new hollow sections such as rectangular or elliptical shapes have been introduced in the catalogues of the steel producers, which need further investigation in order to be accessible to practitioners.

At the same time, despite a large amount of fire tests can be found in the literature on CFST columns subjected to concentric axial load or moderated eccentricities, test results which account for large eccentricities cannot easily be found [11]. Thus, it is needed to extend the experimental database to include the effect of large eccentricities in slender CFST columns. In this paper, rectangular and elliptical concrete-filled tubular columns subjected to both concentric and eccentric loads will be investigated, in order to fill the current void.

Traditionally, circular and square hollow sections have been used in combination with concrete to form composite structural elements – i.e. concrete-filled tubes –, being the major compressive components in buildings or bridges [12]. However, it is less frequent to find in practice elliptical or rectangular hollow sections filled with concrete.

Although the use of elliptical hollow sections (EHS) in construction is growing and these new sections are becoming more popular amongst designers [13][14][15], very few applications can be found where EHS have been filled with concrete, since the design codes for composite members do not cover this new shape. Only the example of the bracing members used in the NEO Bankside residential development in London (UK) can be cited [16]. Therefore, further research is needed in order to establish the structural behaviour of concrete-filled elliptical and rectangular hollow sections and to subsequently develop new design guidance which can be incorporated to the current building codes.

Regarding the fire behaviour of CFST columns, rectangular sections have seldom been studied, being very limited the number of experimental investigations which can be found in the literature, some of which are summarized next.

Han and co-workers [17] tested a total of eight concrete-filled rectangular hollow section (RHS) columns, varying the steel tube depth-to-width ratio, column slenderness and load eccentricity. It was proved that the fire resistance of the columns can be enhanced through the use of fire-protection coat. This group also tested the residual strength of six rectangular columns after exposure to ISO-834 standard fire [18]. It was found that the loss of strength of the specimens without protection was significantly greater than that of columns with fire protection. It was also observed that the slenderness ratio, sectional dimensions and fire exposure time have a significant influence on the residual strength of such columns.

Jiang et al. [19] also studied the residual behaviour of rectangular concrete-filled steel tubular columns. Fourteen specimens which had been exposed to constant high temperatures were subsequently subjected to bi-axial force and bending. This investigation showed that rectangular concrete-filled steel tubular columns still have relatively high carrying capacity and ductility after being exposed to high temperature.

More recently, Yang et al. [20] studied the performance of concrete-filled RHS columns exposed to fire on three sides. Three rectangular columns were tested to failure, two of which were exposed on three sides and the other on four sides. It was found that the shift of the centre of stiffness and the thermal bowing, associated to the asymmetric fire conditions, promote the buckling of the columns.

The available investigations on concrete-filled EHS columns at elevated temperatures are even more limited. Some experimental programmes at room temperature have been carried out in recent years, such as those from Yang et al. [21], Zhao and Packer [22], Sheehan et al. [23] and Jamaluddin et al. [24], which have helped to establish the compressive behaviour of such columns at ambient conditions. In turn, the fire behaviour of these columns has been numerically examined by the own authors [25] and by Dai and Lam [26], comparing their fire performance with other section shapes. Some work on unfilled EHS columns subjected to hydrocarbon fire carried out by Scullion et al. [27] can be also cited. However, very limited experimental results are available on concrete-filled EHS columns exposed to fire, from previous tests performed by the authors of this paper [28]. Therefore, the need of carrying out more fire tests is plenty justified.

The experiments presented in this paper form part of the fire testing program carried out in the framework of the European Project FRISCC (Fire resistance of innovative and slender concrete filled tubular composite columns), which aims at providing a full range of experimental evidence on the fire behaviour of CFST columns as a basis for the development of numerical models and simple calculation rules. Four different section shapes are studied in the mentioned project: circular, elliptical, square and rectangular hollow section columns filled with concrete. The results of the circular and square columns were presented in a previous paper by the authors [29], while the present paper contains the results of the rectangular and elliptical column tests.

The present paper investigates the fire behaviour of slender CFST columns with rectangular and elliptical cross-section, subjected to both concentric and eccentric load, reaching large eccentricities. The effect of the load eccentricity and percentage of reinforcement is studied, considering both major and minor axis eccentricity.

The results from this experimental investigation are also used for evaluating the current simple calculation method in Eurocode 4 Part 1.2 [30]. Previous investigations for concrete-filled CHS and SHS columns by the authors [31][32] and other groups [33] have revealed that this method produces unsafe results for a certain range of slenderness under concentric loads. In this work, the current method will be applied to rectangular and elliptical columns, in order to investigate if these findings hold true also for these shapes, and to evaluate the influence of the effect of the load eccentricity.

2. EXPERIMENTAL INVESTIGATION

2.1. General

This paper presents the results of part of the experimental program carried out in the framework of the European project FRISCC, comprising a total of 18 columns, twelve of them having rectangular section and the other six with elliptical section. The reason of having a more limited number of elliptical sections was due to the difficult commercial availability of these shapes. Two different cross-sectional dimensions were used for the rectangular columns – 250×150×10 (R1-R6) and 350×150×10 (R7-R12) –, while for the elliptical columns one section was analysed – 320×160×12.5 (E7-E12) –. For each shape, two columns were subjected to concentric load, other two tested under eccentric load applied about their minor axis, and two with major axis eccentricity, using load eccentricity ratios (e/H or e/B) of 0.2

and 0.5. Reinforcement was used in some of the columns, using reinforcement ratios around 2.5%. All the columns were hinged at both ends, having a length of 3180 mm. The steel tubes had a nominal strength of 355 MPa, while the concrete used for filling the columns had a compressive strength of 30 MPa. The load level applied to the columns was a 20% of their load bearing capacity at room temperature, which had been calculated by means of a previously validated numerical model.

The sectional dimensions of the elliptical columns E7-E12 were selected so as to have approximately the same steel area than their rectangular counterparts R7-R12 (i.e. same quantity of steel A_a), in order to be able to compare their effectiveness in the fire situation for the same steel usage. However, due to the limitations in the availability of the steel hollow sections in the market, an exact equivalence between rectangular and elliptical columns was not possible to obtain, having an unavoidable difference of a 7.5% in steel area. Note that the numbering of the elliptical specimens has been assigned so that they correspond to their equivalent rectangular counterparts.

The geometrical parameters, material data and resulting fire resistance of all the tested specimens are listed in Table 1 for rectangular columns and Table 2 for elliptical columns. The cross-sectional dimensions and reinforcement arrangement of the tested columns can be seen in Fig. 1.

2.2. Test setup

The fire tests were performed in the facilities of AIDICO (Instituto Tecnológico de la Construcción) in Valencia (Spain), using a 5×3 m furnace equipped with a hydraulic jack with a maximum capacity of 1000 kN and a total of 16 gas burners, located at mid-height of the furnace chamber. Fig. 2 presents a schematic view of the experimental setup.

Knife-edge bearings were attached to both column ends, which permitted to apply the desired eccentricity. The columns were loaded through their top end, and, once the load was applied, it was kept constant while the standard ISO-834 [34] fire curve was prescribed, with unrestrained column elongation.

2.3. Column specimens

The length of the columns was 3180 mm, although only 3040 mm were directly exposed to the fire inside the furnace.

A 300×300×15 mm steel plate was welded to the bottom end of the columns. The columns were then put in an upright position and filled with concrete, and afterwards shaken by means of an external vibrator in order to consolidate the concrete inside the steel tube. The columns were sealed with plastic at their top ends in order to avoid moisture leaks and left upright for 28 days. After concrete was cured, the top surface of the columns was polished and a second end plate of the same dimensions was then welded to the top end of the columns. For each column specimen, two vent holes of 15 mm diameter were drilled in the steel hollow section wall at 100 mm from each column end. These vent holes were provided for relieving the water vapour pressure produced during the experiment. An additional hole, located near the bottom end of the columns, was used for connecting the thermocouple wires.

2.4. Instrumentation

In order to register the temperature evolution inside the columns during the fire tests, three layers of seven thermocouples each were placed at different heights, as it can be seen in Fig. 2 (section A-A': L/2, section B-B': L/4, section C-C': 3L/4). The thermocouple location at each section can be seen in Fig. 3 (TC1 to TC7) for the two geometries studied. TC1 and TC6 were located at the steel tube exposed surface, while the other 5 thermocouples (TC2 to TC5 and TC7) were embedded in the concrete core.

The temperature inside the furnace chamber was automatically registered and controlled during the tests by means of 6 plate thermocouples and a pressure sensor. The plate thermocouples were located at sections A-A', B-B' and C-C' in pairs as indicated in Fig. 2. The axial elongation at the top end of the columns was measured during the tests by means of a LVDT located outside the furnace.

2.5. Material properties

The hollow tubes used in the experimental program were produced with S355 steel grade, nevertheless the real strength (f_y) of steel was obtained by performing the corresponding coupon tests, and is summarized in Table 1 and Table 2. It is worth noting that the measured yield strength of the elliptical tubes resulted remarkably high.

Normal strength concrete (30 MPa) was used for the column infill. In order to determine the compressive strength of concrete, sets of concrete cylinders were prepared and cured in standard conditions during 28 days. All cylinder samples were tested on the same day as the column fire test. The cylinder compressive strength of all the tested specimens (f_c) can be found in Table 1 and Table 2. The bar-reinforced specimens had the arrangements shown in Fig. 1 using 6 mm stirrups with 30 cm spacing. The corresponding geometrical reinforcement ratios ($\rho = A_s/A_c$) and measured yield strength (f_s) are given in Table 1 and Table 2.

In order to measure the concrete moisture content, cubic specimens of 150×150×150 mm were also prepared. The moisture content was obtained according to the procedure described in ISO 12570:2000 [35].

3. ANALYSIS OF RESULTS

3.1. Thermal response

The evolution of temperatures at mid-height section for one of the columns tested (specimen E10) can be observed in Fig. 4. TC1 and TC6, located at the steel tube outer surface, lie close to each other and follow the shape of the furnace curve with a certain delay, reaching 600ºC between 15 and 20 minutes. In turn, the temperatures measured at the concrete core (TC2-TC5, TC7) are significantly lower, being observed a decrease in the heating rate between 100ºC and 200ºC due to the heat consumption by water evaporation. TC2 and TC7, closer to the steel-concrete interface, register higher temperatures from the beginning of the test – although with important oscillations during the evaporation phase –, while TC4, located at the center of the section provides the lower measurements.

3.2. Mechanical response

The typical failure mode observed in these series of tests was overall buckling, which can be observed in Fig. 5 for some of the specimens tested. Local buckling was also observed at mid-height in most of the rectangular columns. For some of the columns with eccentricity applied about the major axis, interaction between major and minor axis occurred (i.e. the curvature of the column was significant in both planes), mainly in those cases with moderated eccentricity (0.2H), see Fig. 5b, while for those cases with eccentricity 0.5H the column clearly buckled about its major axis, see Fig. 5a.

The results of the fire tests are presented in this paper in the form of axial displacement versus time curves, grouped in different graphs according to their cross-section shape and dimensions. Fig. 6 corresponds to the rectangular columns, while Fig. 7 corresponds to the elliptical columns. The evolution of the axial displacement measured at the top end of the columns versus the fire exposure time was registered during the fire tests and is presented in these figures. Note that in the second series of rectangular columns (Fig. 6b), the results of specimens R7 and R12 have been marked as anomalous, and should not be used for comparison. In the case of test R7, some of the gas burners failed, causing that the average furnace temperature was lower that the reference ISO-834 standard fire curve, therefore leading to fire resistance time higher than expected. Contrarily, in test specimen R12 a gap was formed near the mid-height section during the concrete casting, leaving a considerable area of the hollow steel tube unfilled and thus causing the column to buckle prematurely.

Due to the high slenderness of the columns, combined with large eccentricities, only two stages were observed in the axial displacement versus time curves: axial elongation of the column and sudden failure after the yielding of the steel tube occurred, thus not taking advantage of the contribution of the concrete core, which in typical tests for specimens with more reduced slenderness was reflected as a plateau in these curves [4][9].

The resulting fire resistance time expressed in minutes, obtained according to the failure criteria in EN 1363-1 [36] is listed in Table 1 for the rectangular columns and Table 2 for the elliptical columns. Fig. 8 compares the elliptical and rectangular specimens in terms of steel area, fire resistance, applied load and member slenderness, in order to facilitate the subsequent analysis.

The influence of the load eccentricity can be observed in the presented figures, for both major and minor axis. It can be observed that, as the load eccentricity was increased, the fire resistance time also increased, which was due to the differences on the applied load. In effect, as the load level applied to all the columns was the same (20% of their theoretical maximum capacity at room temperature), the value of the load applied to the columns with higher eccentricity was lower, and therefore the resulting fire resistance time was higher. However, it results more useful to see this comparison in terms of load increment. For instance, if column specimens R2 (axially loaded) and R4 (eccentricity 0.5B) are compared, with the same column dimensions and reinforcement, it can be seen that the load applied to the concentrically loaded column was around 2.5 times the load applied to the eccentrically loaded column, while the difference in terms of fire resistance time was not proportional to the load increment (17.4% difference in terms of failure time).

The effect of the eccentricity applied about the major axis can be observed by comparing case R1 against R5 and R6 (Fig. 6a), with the same column dimensions and relative eccentricities of 0, 0.2H and 0.5H. As it can be seen, the fire resistance time also increased when applying increasing eccentricities on the major axis, due to the reduction in the applied load. This behaviour can be also noticed in the elliptical columns, comparing case E7 against E11 and E12 (Fig. 7). It should be noted that the load applied to the concentrically loaded columns was about two times the load applied to the columns with 0.5H relative eccentricity.

Comparing between reinforced and unreinforced specimens, it can be seen that, although the load applied to the reinforced specimens was higher, the values of their fire resistance times were similar or in some cases higher than those of the unreinforced columns (see R1/R2), which confirms the slightly favourable effect of the contribution of the reinforcing bars in the fire situation.

If the elliptical series E7-E12 is compared against the rectangular series R7-R12, having a similar steel area (7.5% difference) – see quantitative comparison given in Fig. 8 – the elliptical columns achieve a higher fire resistance time (44.4% higher on average, discarding cases R7 and R12), although it should be noted that the loads applied to the rectangular columns were higher to those applied to the elliptical columns, with a 50.9% average increment. Therefore, in this case it is difficult to reach a conclusion in favour of one or other section shape. Further studies are needed for obtaining a conclusive result, which the authors will carry out in the future by means of numerical simulations.

4. STUDY AND DISCUSSION OF EUROCODE 4

The fire resistance of columns composed of unprotected concrete-filled square or circular hollow sections can be assessed following the rules in Clause 4.3.5.3 of EN 1994-1-2 [30], which refers to Annex H for a specific calculation method. In turn, Clause 4.3.5.1 of the same code provides a general method for composite columns. The method in Annex H is currently under revision due to its proved unsafety for slender columns, and alternatively it is recommended to use the general method in Clause 4.3.5.1, as given in the National Annexes and design guides published by a number of countries (e.g. United Kingdom [37]). This method has been tested for circular and square columns in previous investigations [31][32][33], giving place to a debate on the values of certain coefficients which still need to be specified for CFST columns. However, columns with rectangular or elliptical cross-section are not frequently considered in the evaluation of the method. This section aims at evaluating the accuracy of the simple calculation model in Clause 4.3.5.1 of EN 1994-1-2 for these new geometries, which will be the basis for the development of a design method within the European project FRISCC.

4.1. Concentric load

Clause 4.3.5.1 presents a method for calculating the design value of the buckling resistance of composite columns subjected to concentric axial loads in the fire situation, based on the elastic buckling theory. In this simple calculation model, the design value of the resistance of composite columns in axial compression exposed to fire ($N_{fi,Rd}$) is calculated as:

$$N_{fi,Rd} = \chi N_{fi,pl,Rd} \tag{1}$$

where χ is the reduction coefficient for buckling curve “c” given in Clause 6.3.1.2 of EN 1993-1-1 (obtained from the value of the relative slenderness at elevated temperature) and

$N_{fi,pl,Rd}$ is the design value of the plastic resistance of the cross-section to axial compression in fire.

The design value of the plastic resistance of the cross-section in the fire situation ($N_{fi,pl,Rd}$) is given by:

$$N_{fi,pl,Rd} = \sum_j (A_{a,\theta} f_{ay,\theta}) / \gamma_{M,fi,a} + \sum_k (A_{s,\theta} f_{sy,\theta}) / \gamma_{M,fi,s} + \sum_m (A_{c,\theta} f_{c,\theta}) / \gamma_{M,fi,c} \quad (2)$$

where $A_{i,\theta}$ is the area of each element of the cross-section to which a certain temperature θ is attributed and subscripts "a", "s" and "c" refer to the steel profile, reinforcing bars and concrete core, respectively. $\gamma_{M,fi,i}$ are the partial factors for the materials in the fire situation.

The effective flexural stiffness of the column can be calculated through:

$$(EI)_{fi,eff} = \sum_j (\varphi_{a,\theta} E_{a,\theta} I_{a,\theta}) + \sum_k (\varphi_{s,\theta} E_{s,\theta} I_{s,\theta}) + \sum_m (\varphi_{c,\theta} E_{c,\sec,\theta} I_{c,\theta}) \quad (3)$$

where $I_{i,\theta}$ is the second moment of area of each element of the cross-section to which a certain temperature θ is attributed, $\varphi_{i,\theta}$ is the reduction coefficient depending on the effect of thermal stresses and $E_{c,sec,\theta}$ is the secant modulus of concrete at the temperature θ.

The evaluation of this equation requires the definition of a set of reduction coefficients ($\varphi_{i,\theta}$) to account for the effect of the thermal stresses. However, for concrete-filled sections, the values of these reduction coefficients are not specified in the code. In the absence of predefined values for these coefficients, a common approach in practice is to take them as equal to unity [38]. Another assumption is to use the values in Annex G of EN 1994-1-2 for composite columns with partially encased steel sections, as recommended in the British design guide for concrete-filled structural hollow section columns [37].

Once the effective flexural stiffness is calculated, the Euler buckling load in the fire situation is obtained as follows:

$$N_{fi,cr} = \pi^2 (EI)_{fi,eff} / \ell_\theta^2 \quad (4)$$

where ℓ_θ is the effective length of the column at a certain temperature

The relative slenderness of the column at elevated temperatures is given by:

$$\bar{\lambda}_\theta = \sqrt{N_{fi,pl,R} / N_{fi,cr}} \tag{5}$$

where $N_{fi,pl,R}$ is the value of $N_{fi,pl,Rd}$ when the material factors are taken as 1.0.

This value of the relative slenderness is used to enter to the buckling curve “c”, from where the reduction coefficient χ needed for determining the buckling load is finally obtained.

4.2. Eccentric load

For eccentric loads, reference is made in Clause 4.3.5.3 to Section H.4 in Annex H of EN 1994-1-2, specific for circular and square CFST columns. Two correction coefficients are given in Figures H.1 and H.2 of the referred Annex (see Fig. 9): φ_s, as function of the percentage of reinforcement, and φ_δ, as function of the eccentricity and the slenderness of the column.

$$N_{fi,Rd,\delta} = N_{fi,Rd} \cdot \varphi_s \cdot \varphi_\delta \tag{6}$$

In this equation, the buckling resistance of the column under concentric axial load $N_{fi,Rd}$ is firstly evaluated and, afterwards, it is corrected by means of the two coefficients φ_s and φ_δ, for obtaining the eccentric buckling load $N_{fi,Rd,\delta}$.

Note that the coefficient φ_δ depends on the ratios ℓ_θ/B and δ/B, being B the size of a square section, while in this paper the columns analyzed are of rectangular and elliptical cross-section. Therefore, an assumption must be done when applying the graph in Figure H.2 of EN 1994-1-2 (Fig. 9b in this paper). For the purpose of the calculations in this paper, the dimension H or B parallel to the loading axis has been used ℓ_θ/B - δ/B for minor axis bending and ℓ_θ/H - δ/H for major axis bending.

Section G.7 of Annex G, for composite columns with partially encased steel sections presents a totally different approach, where the design fire buckling load with eccentricity

$N_{fi,Rd,\delta}$ is calculated from the concentric axial buckling load in the fire situation $N_{fi,Rd}$ corrected by means of the relation between these two loads at room temperature, as follows:

$$N_{fi,Rd,\delta} = N_{fi,Rd} \left(N_{Rd,\delta} / N_{Rd} \right) \tag{7}$$

4.3. Application of the simple calculation model in Eurocode 4 to the tested columns

In this section, the simple calculation model from Clause 4.3.5.1 in EN 1994-1-2 is applied to the tested specimens, and the predictions compared with the test results from the experimental program.

The application of these methods requires the previous calculation of the temperature field of the composite cross-section at the time of failure. For that purpose, the column cross-section is subdivided into a number of concentric layers of the same thickness, as can be seen in Fig. 10. Using the measured temperatures at the locations of the thermocouples, the temperature of each layer is obtained by means of linear interpolation.

After obtaining the temperature field at the time of failure, the design axial buckling load $N_{fi,Rd}$ is calculated as explained in Section 4.1. Two different approaches are used for evaluating the effective flexural stiffness given in eq. (3): using unity coefficients $\varphi_{i,\theta}$, [38] or alternatively taking the values of these coefficients from Table G.7 in Annex G [37].

In the case of eccentrically loaded columns, the buckling load $N_{fi,Rd,\delta}$ is calculated as described in Section 4.2, by correcting the axial buckling load $N_{fi,Rd}$ by means of two options: using the correction coefficients from Section H.4 in Annex H (eq. 6) or using the relation between the eccentric capacity and axial capacity at room temperature, as given in Section G.7 of Annex G (eq. 7).

Table 3 and Table 4 compare the predictions of the simple calculation method for rectangular and elliptical columns, respectively, with the test results. Table 3a and Table 4a correspond to concentrically loaded columns, while Table 3b and Table 4b present the results of the eccentrically loaded columns. In these tables, the prediction error is defined as the test load divided by the calculated load. These comparisons between calculated load and test load can be also seen in Fig. 11 for rectangular columns and Fig. 12 for elliptical columns. Note that case specimens R7 and R12 do not provide reliable results, since these fire tests were anomalous.

Evaluating the results in the presented tables and figures, it can be seen that, for concentrically loaded columns, the simple calculation method provides unsafe results for both rectangular and elliptical columns, using unity coefficients or alternatively those values given in Annex G. In the case of rectangular columns, an average error of 0.64-0.66 is obtained, depending on the coefficients used, while for elliptical columns 0.86-0.89 average error is found. This confirms that the general method in Clause 4.3.5.1 produces unsafe results for concentrically loaded slender columns, as found in previous investigations [31][32]. Therefore, a set of reduction coefficients $\varphi_{i,\theta}$ should be developed so that the simple calculation model can be safely applied to concentrically loaded rectangular and elliptical columns.

For eccentrically loaded columns, two options have been considered: using the correction coefficients from Section H.4 or the approach in Section G.7 based on the relation of ultimate loads at room temperature. For rectangular columns, the former option provides safe results (1.63-1.68), while the latter gives place to unsafe predictions (0.82-0.85). For elliptical columns, the first option also provides safe results (2.04-2.13), while the second option provides more accurate results, close to the experimental values (0.99-1.04) and with a very reduced dispersion (standard deviation of 0.05). Therefore, it seems that the second approach can be applied to elliptical columns with reasonable results, while for rectangular columns it should be corrected so as to obtain safer results. What is remarkable in any case is that this second approach provides more uniformity in the predictions, with a lower standard deviation in all the cases, therefore it is suggested that a proposal for the calculation of the eccentric capacity at elevated temperature based on the relation of ultimate loads at room temperature is developed.

It should be noted that, for unreinforced columns subjected to eccentric loads (R3-R5-R9-R11, E9-E11), too conservative predictions are obtained with the first approach, correction from Section H.4 – with errors ranging between 1.60 and 3.20 – due to the low value of the correction coefficient φ_s from Figure H.1 of EN 1994-1-2 (see Fig. 9a), which for unreinforced columns is equal to 0.4. However, for reinforced columns, this coefficient increases up to 0.9 for the percentages of reinforcement used in the tested columns (ρ = 2.57% - 2.69%), producing results which are still safe but less conservative. This finding confirms the observations from previous investigations by the authors [10]: the application of these correction coefficients produces excessively safe-sided results for unreinforced columns, while for reinforced columns more realistic results can be obtained.

Therefore, the correction coefficients φ_s and φ_δ to account for the effect of the eccentricity should be revised, so that a higher precision and uniformity in the predictions for both reinforced and unreinforced columns can be obtained. New equations and graphs are needed, which will be developed in the future based on the parametric studies carried out in the framework of the European project FRISCC.

Summing up, in order to improve the accuracy of the simple calculation method in EN 1994-1-2 and extend its applicability to rectangular and elliptical columns, a set of reduction coefficients $\varphi_{i,\theta}$ should be developed for evaluating the effective flexural stiffness of the columns, as well as a correction method for taking into account the effect of the load eccentricity, either through coefficients in the form of those given in Section H.4 or alternatively using the relation of ultimate loads at room temperature as done in Section G.7.

5. SUMMARY AND CONCLUSIONS

The results of an experimental program on rectangular and elliptical concrete-filled tubular columns under elevated temperatures have been presented in this paper. The columns were subjected to concentric and eccentric loads about both minor and major axis, reaching large eccentricities of 0.5 times the sectional dimensions. A total of twelve rectangular columns and six elliptical columns were tested under pinned-ended conditions and subjected to a 20% load level, being exposed to the standard ISO-834 fire curve.

Analysing the experimental results, it was found out that the eccentricity had a detrimental effect on the fire resistance time, while the presence of reinforcing bars contributed to increase the load-bearing capacity of the columns in the fire situation. Interaction between major and minor axis was observed in those specimens loaded with moderated eccentricity about their major axis (0.2H), while for those cases with 0.5H eccentricity the columns buckled primarily about their major axis. In general, the elliptical columns achieved a higher fire resistance time than their rectangular counterparts with the same steel usage, although since the loads applied to the rectangular columns were higher to those applied to the elliptical columns, it was difficult to reach a conclusion in favour of one or other section shape.

Based on the experimental results, the simple calculation model in Clause 4.3.5.1 of EN 1994-1-2 was evaluated for elliptical and rectangular columns. It was found that, the simple calculation model leads to unsafe predictions for concentrically loaded columns, regardless the values of the reduction coefficients used for calculating the effective flexural stiffness. In turn, for eccentrically loaded columns, two options were considered, leading to different results. When the correction coefficients from Section H.4 were used, safe results were obtained, although too conservative for the case of unreinforced columns. If the correction from Section G.7 was considered, unsafe predictions were obtained for the rectangular columns, while for elliptical columns the results were more accurate. This second approach resulted in more uniform predictions, therefore it is suggested that the calculation of the eccentric capacity at elevated temperature is based on the relation at room temperature rather than using the correction coefficients from Section H.4, although a new proposal should be developed in order to obtain safe predictions for both geometries.

Also the flexural stiffness reduction coefficients should be revised in order to safely apply the simple calculation model in Clause 4.3.5.1 for elliptical and rectangular columns. This will be done shortly on the basis of the parametric studies to be carried out within the European Project FRISCC.

ACKNOWLEDGEMENTS

The authors would like to express their sincere gratitude to the European Union for the help provided through the Project RFSR-CT-2012-00025, carried out with a financial grant of the Research Programme of the Research Fund for Coal and Steel.

REFERENCES

[1] COMETUBE. Fire resistance of structural hollow sections. Cometube research. CIDECT programme 15A. Final report; 1976.

[2] Grandjean G, Grimault JP, Petit L. Determination de la duree au feu des profils creux remplis de beton. CIDECT Research Project 15B–80/10. Cologne, Germany: Comité International pour le Développement et l'Etude de la Construction Tubulaire; 1980.

[3] Kordina K, Klingsch W. Fire resistance of composite columns of concrete filled hollow sections. CIDECT Research Project 15C1/C2–83/27. Cologne, Germany: Comité International pour le Développement et l'Etude de la Construction Tubulaire; 1983.

[4] Lie TT, Chabot M. Experimental studies on the fire resistance of hollow steel columns filled with plain concrete. Internal report No. 611. Ottawa, Canada: Institute for Research in Construction, National Research Council of Canada (NRCC); 1992.

[5] Chabot M, Lie TT. Experimental studies on the fire resistance of hollow steel columns filled with bar-reinforced concrete. Internal report No. 628. Ottawa, Canada: Institute for Research in Construction, National Research Council of Canada (NRCC); 1992.

[6] Kodur VKR, Lie TT. Experimental studies on the fire resistance of circular hollow steel columns filled with steel-fibre-reinforced concrete. Internal report No. 691. Ottawa, Canada: Institute for Research in Construction, National Research Council of Canada; 1995.

[7] Han LH, Zhao XL, Yang YF, Feng JB. Experimental study and calculation of fire resistance of concrete-filled hollow steel columns. Journal of Structural Engineering (ASCE) 2003; 129(3):346-356.

[8] Kim DK, Choi SM, Kim JH, Chung KS, Park SH. Experimental study on fire resistance of concrete-filled steel tube column under constant axial loads. International Journal of Steel Structures 2005; 5(4):305-313.

[9] Romero ML, Moliner V, Espinos A, Ibañez C, Hospitaler A. Fire behavior of axially loaded slender high strength concrete-filled tubular columns. Journal of Constructional Steel Research 2011; 67(12):1953-1965.

[10] Moliner V, Espinos A, Romero ML, Hospitaler A. Fire behavior of eccentrically loaded slender high strength concrete-filled tubular columns. Journal of Constructional Steel Research 2013; 83:137-146.

[11] Renaud C, Kruppa J. Unprotected concrete filled columns fire tests – Verification of 15Q. CIDECT Research Project 15R. Saint-Rémy-lès-Chevreuse, France: Centre Technique Industriel de la Construction Métallique (CTICM); 2004.

[12] Han LH, Li W, Bjorhovde R. Developments and advanced applications of concrete-filled steel tubular (CFST) structures: Members. Journal of Constructional Steel Research 2014; 100:211-228.

[13] Gardner L, Ministro A. Structural steel oval hollow sections. Structural Engineer 83(21):32–36, 2005.

[14] Chan TM, Gardner L, Law KH. Structural design of elliptical hollow sections: a review. Structures and Buildings 163(6):391-402, 2010.

[15] Packer JA. Going elliptical. Modern Steel Construction 48(3):65–67, 2008.

[16] Tata Steel. Structural Case Study: NEO Bankside, London. Northants, United Kingdom; 2012.

[17] Han LH, Yang YF, Xu L. An experimental study and calculation on the fire resistance of concrete-filled SHS and RHS columns. Journal of Constructional Steel Research 2003; 59:427-452.

[18] Han LH, Yang YF, Yang H, Huo JS. Residual strength of concrete-filled RHS columns after exposure to the ISO-834 standard fire. Thin-Walled Structures 2002; 40:991-1012.

[19] Jiang SF, Wu ZQ, Niu DS. Experimental study on fire-exposed rectangular concrete-filled steel tubular (CFST) columns subjected to bi-axial force and bending. Advances in Structural Engineering 2010; 13(4):551–60.

[20] Yang H, Liu F, Gardner L. Performance of concrete-filled RHS columns exposed to fire on 3 sides. Engineering Structures 2013; 56:1986–2004.

[21] Yang H, Lam D, Gardner L. Testing and analysis of concrete-filled elliptical hollow sections. Engineering Structures 2008; 30:3771–81.

[22] Zhao XL, Packer JA. Tests and design of concrete-filled elliptical hollow section stub columns. Thin-Walled Structures 2009; 47:617–28.

[23] Sheehan T, Dai XH, Chan TM, Lam D. Structural response of concrete-filled elliptical steel hollow sections under eccentric compression. Engineering Structures 2012; 45: 314–23.

[24] Jamaluddin N, Lam D, Dai XH, Ye J. An experimental study on elliptical concrete filled columns under axial compression Journal of Constructional Steel Research 2013; 87: 6–16.

[25] Espinos A, Gardner L, Romero M, Hospitaler A. Fire behaviour of concrete filled elliptical steel columns. Thin-Walled Structures 2011; 49(2):239-255.

[26] Dai XH, Lam D. Shape effect on the behaviour of axially loaded concrete filled steel tubular stub columns at elevated temperature. Journal of Constructional Steel Research 2012; 73:117-127.

[27] Scullion T, Ali F, Nadjai A. Experimental study on performance of elliptical section steel columns, under hydrocarbon fire. Journal of Constructional Steel Research 2011; 67(6):986-991.

[28] Espinos A, Romero ML, Portolés JM, Hospitaler A. Ambient and fire behaviour of eccentrically loaded elliptical slender concrete-filled tubular columns. Journal of Constructional Steel Research 2014; 100:97-107.

[29] Espinos A, Romero ML, Serra E, Hospitaler A. Circular and square slender concrete-filled tubular columns under large eccentricities and fire. Journal of Constructional Steel Research (under evaluation).

[30] CEN. EN 1994-1-2, Eurocode 4: Design of composite steel and concrete structures. Part 1-2: General rules - Structural fire design. Brussels, Belgium: Comité Européen de Normalisation; 2005.

[31] Espinos A, Romero ML, Hospitaler A. Simple calculation model for evaluating the fire resistance of unreinforced concrete filled tubular columns. Engineering Structures 2012; 42:231-244.

[32] Espinos A, Romero ML, Hospitaler A. Fire design method for bar-reinforced circular and elliptical concrete filled tubular columns. Engineering Structures 2013; 56:384-395.

[33] Aribert JM, Renaud C, Zhao B. Simplified fire design for composite hollow-section columns. Structures & Buildings 2008; 161:325-336.

[34] ISO 834: Fire resistance tests, elements of building construction. Switzerland: International Standards Organisation; 1980.

[35] ISO 12570:2000. Hygrothermal performance of building materials and products - Determination of moisture content by drying at elevated temperature.

[36] CEN. EN 1363-1, Fire resistance tests. Part 1: General requirements. Brussels, Belgium: Comité Européen de Normalisation; 1999.

[37] Wang YC. Design guide for concrete filled hot finished structural hollow section (SHS) columns. TATA Steel; 2014.

[38] Lennon T, Moore DB, Wang YC, Bailey CG. Designers' guide to EN 1991-1-2, EN 1992-1-2, EN 1993-1-2 and EN 1994-1-2. Thomas Telford Limited; 2007.

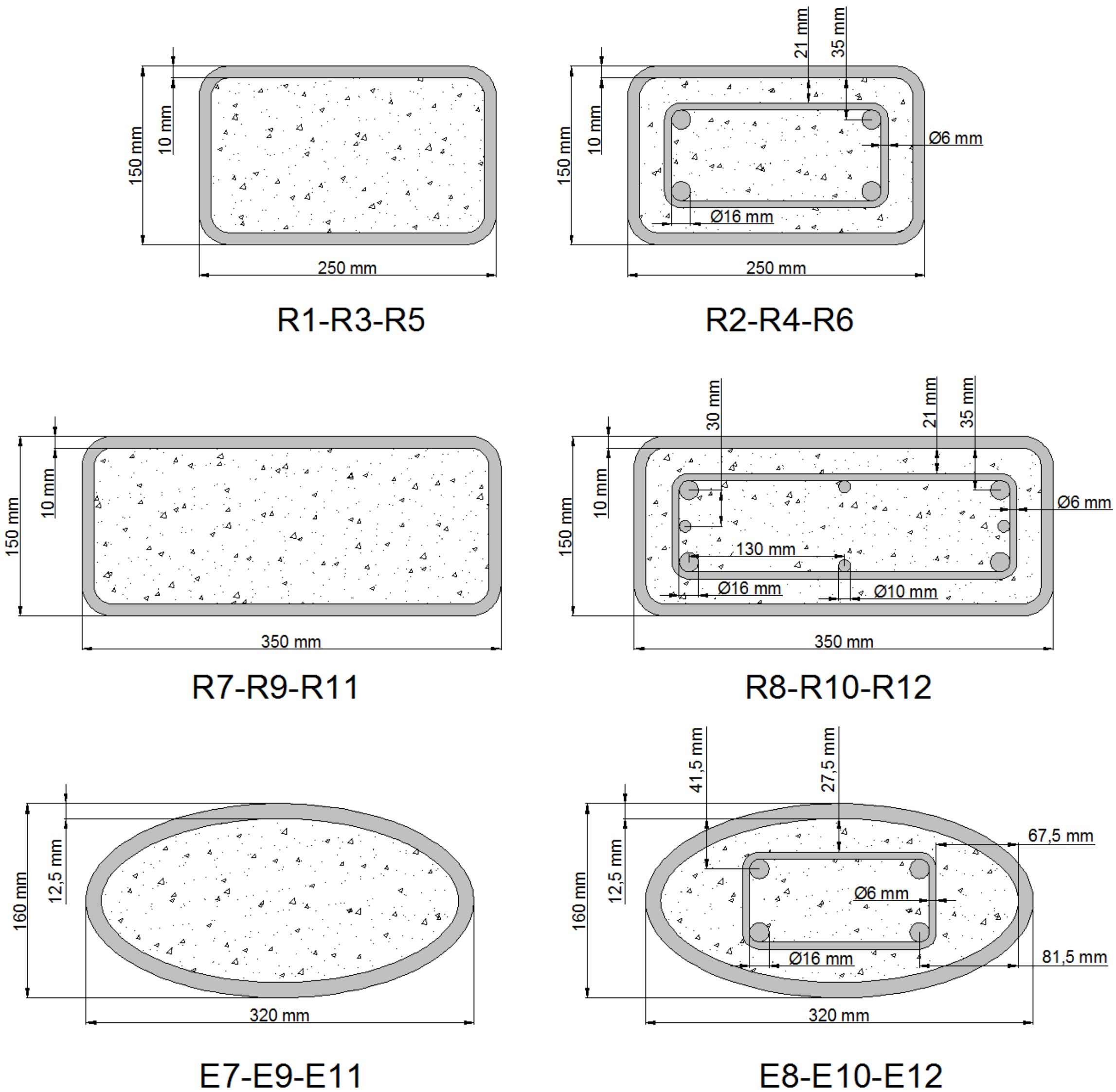

Fig. 1. Cross-sectional dimensions and reinforcement arrangement of the tested columns

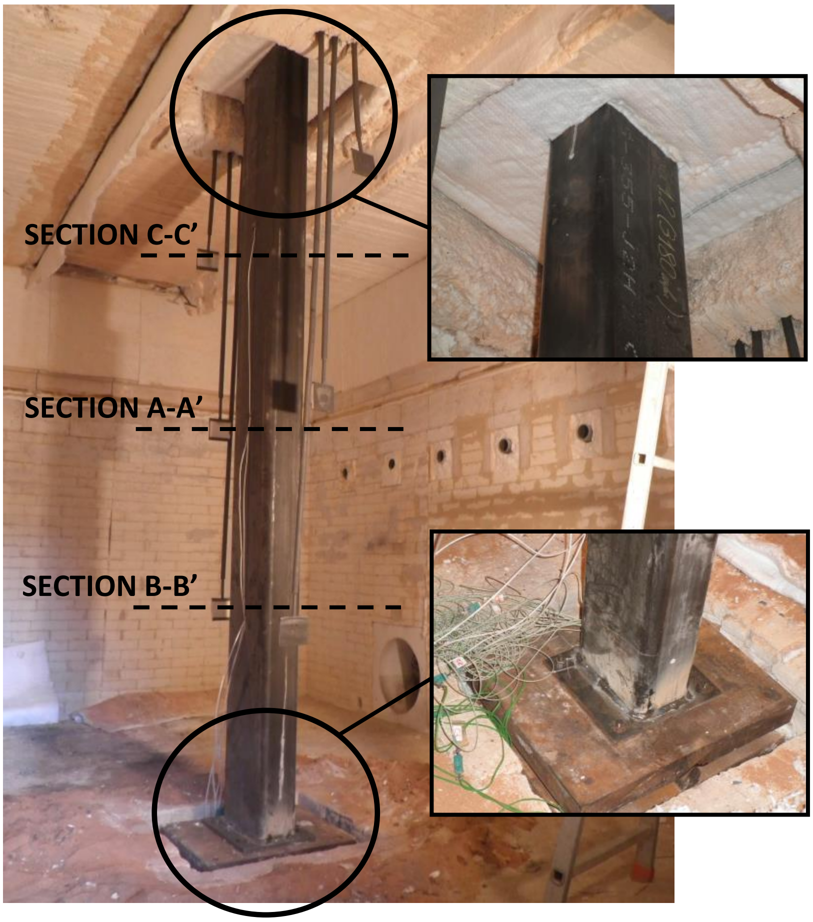

Fig. 2. Test setup and details of the column ends

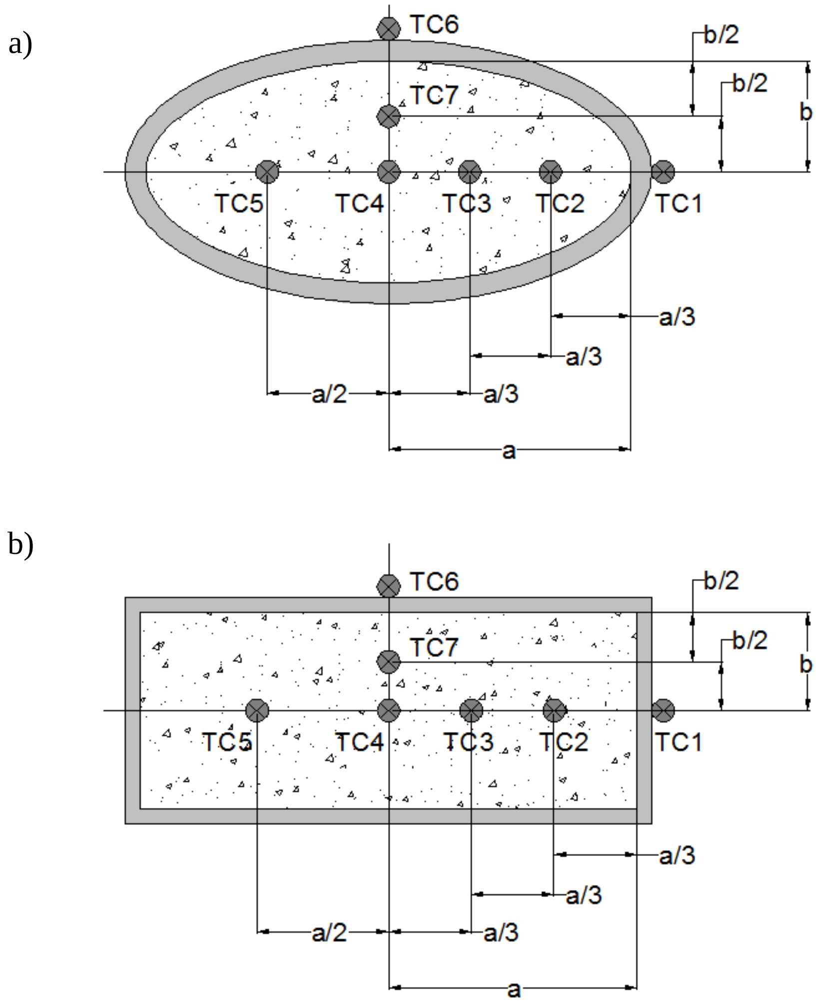

Fig. 3. Thermocouple locations: a) elliptical columns; b) rectangular columns

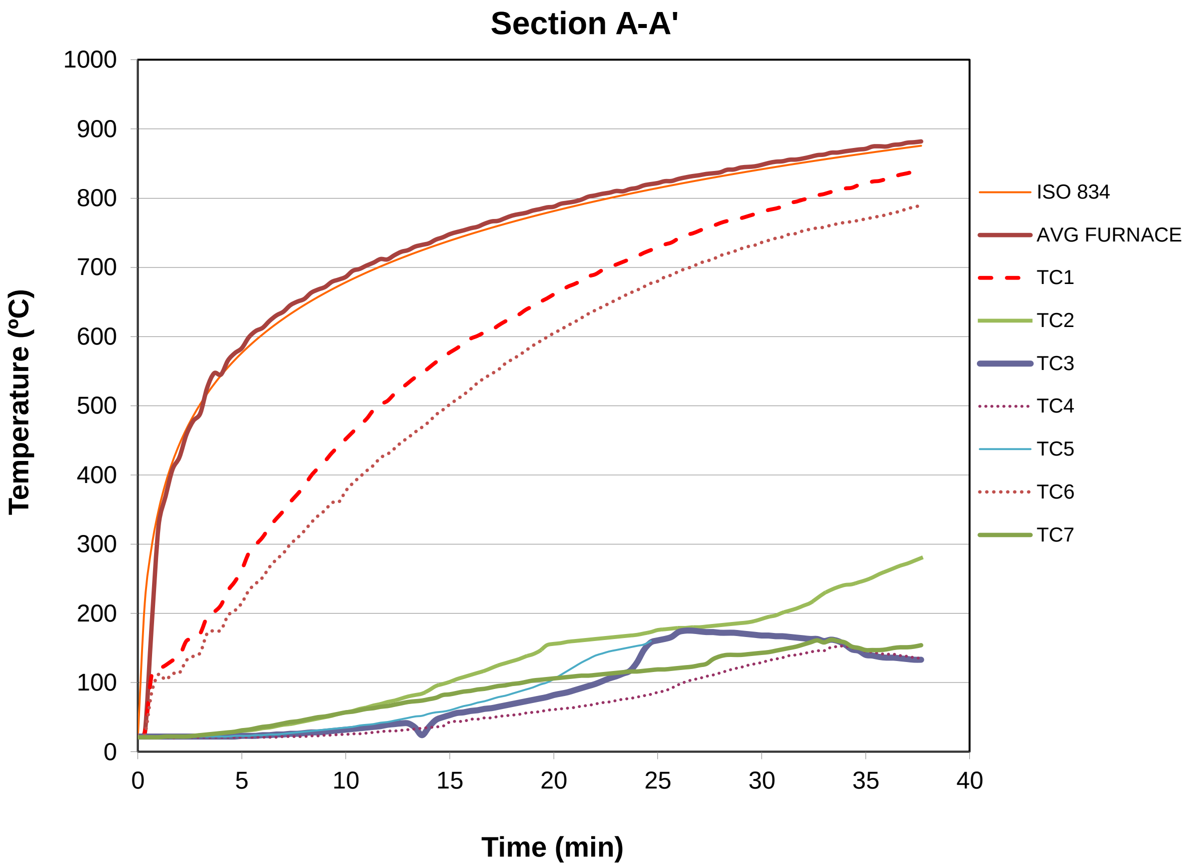

Fig. 4. Evolution of temperatures at mid-height section (A-A’), for column E10.

Fig. 5. View of tested columns after failure: a) column E12 (e/H = 0.5); b) column R11 (e/H = 0.2)

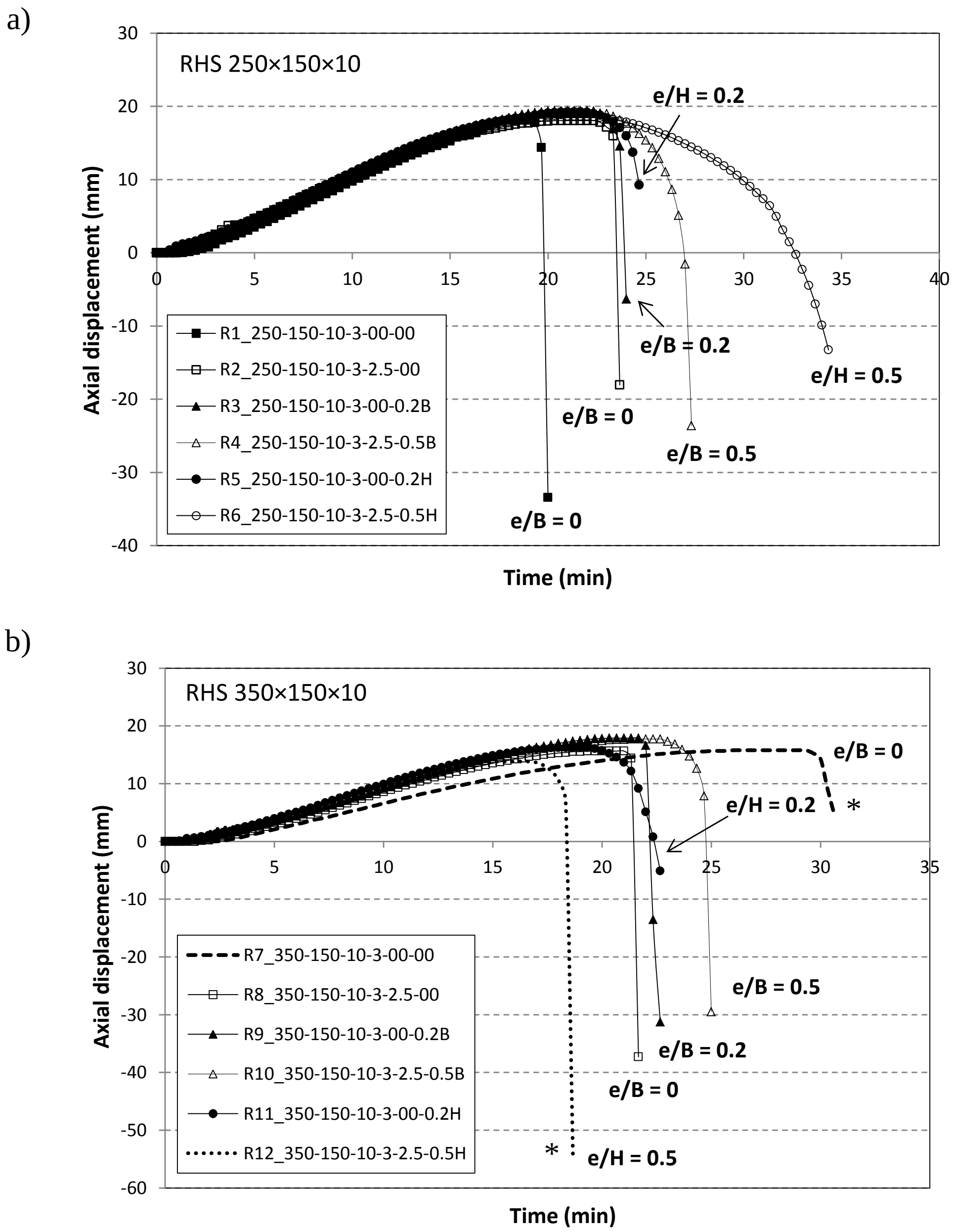

*Anomalous test

Fig. 6. Results of the fire tests on rectangular columns: a) RHS 250×150×10 mm; b) RHS 350×150×10 mm

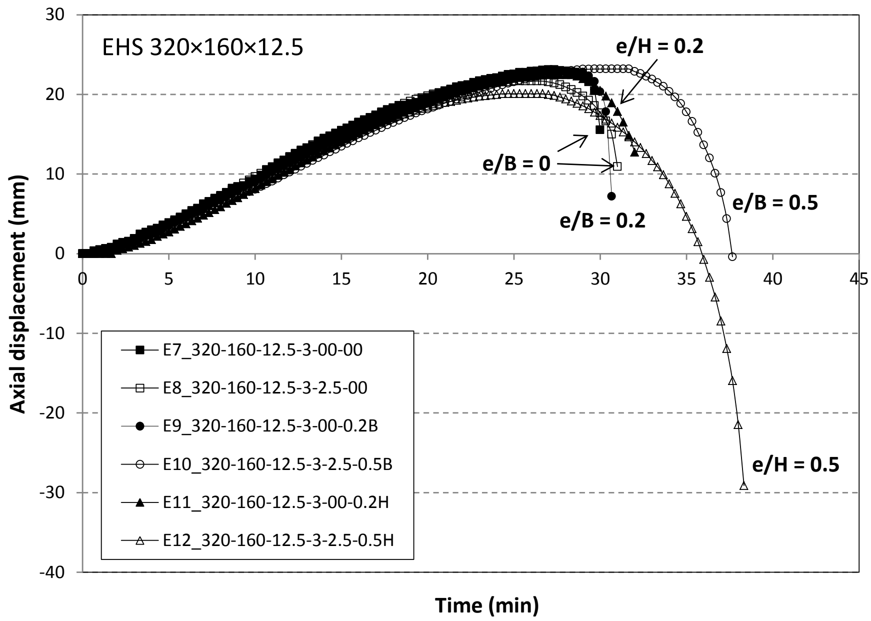

Fig. 7. Results of the fire tests on elliptical columns: EHS 320×160×12.5 mm

Espinos A, Romero ML, Serra E, Hospitaler A. Experimental investigation on the fire behaviour of rectangular and elliptical slender concrete-filled tubular columns. Thin-Walled Struct. 2015;93:137-48. doi: 10.1016/j.tws.2015.03.018

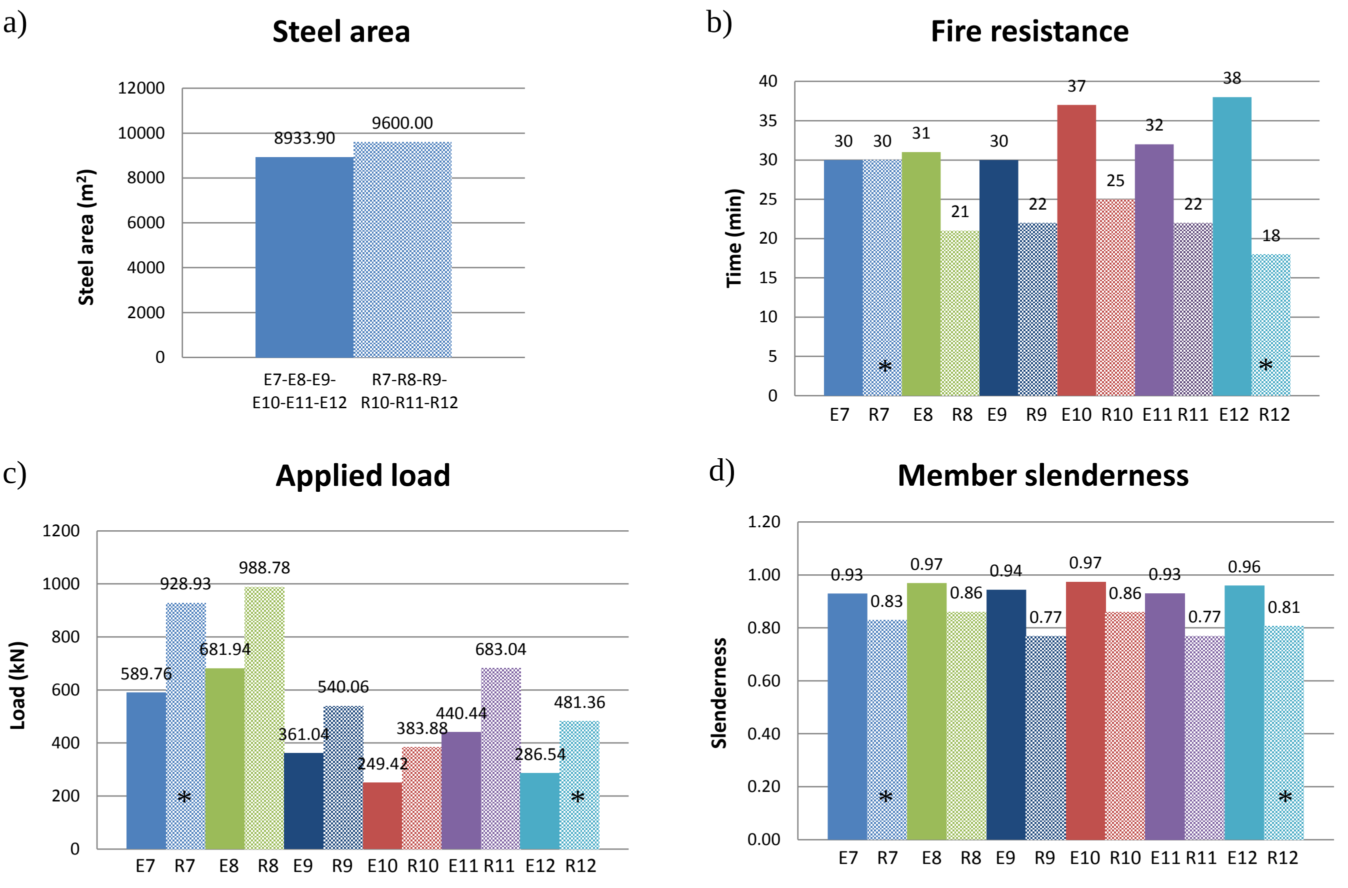

*Anomalous test

Fig. 8. Comparison between rectangular and elliptical columns: a) Steel area; b) Fire resistance time; c) Applied load; d) Member slenderness

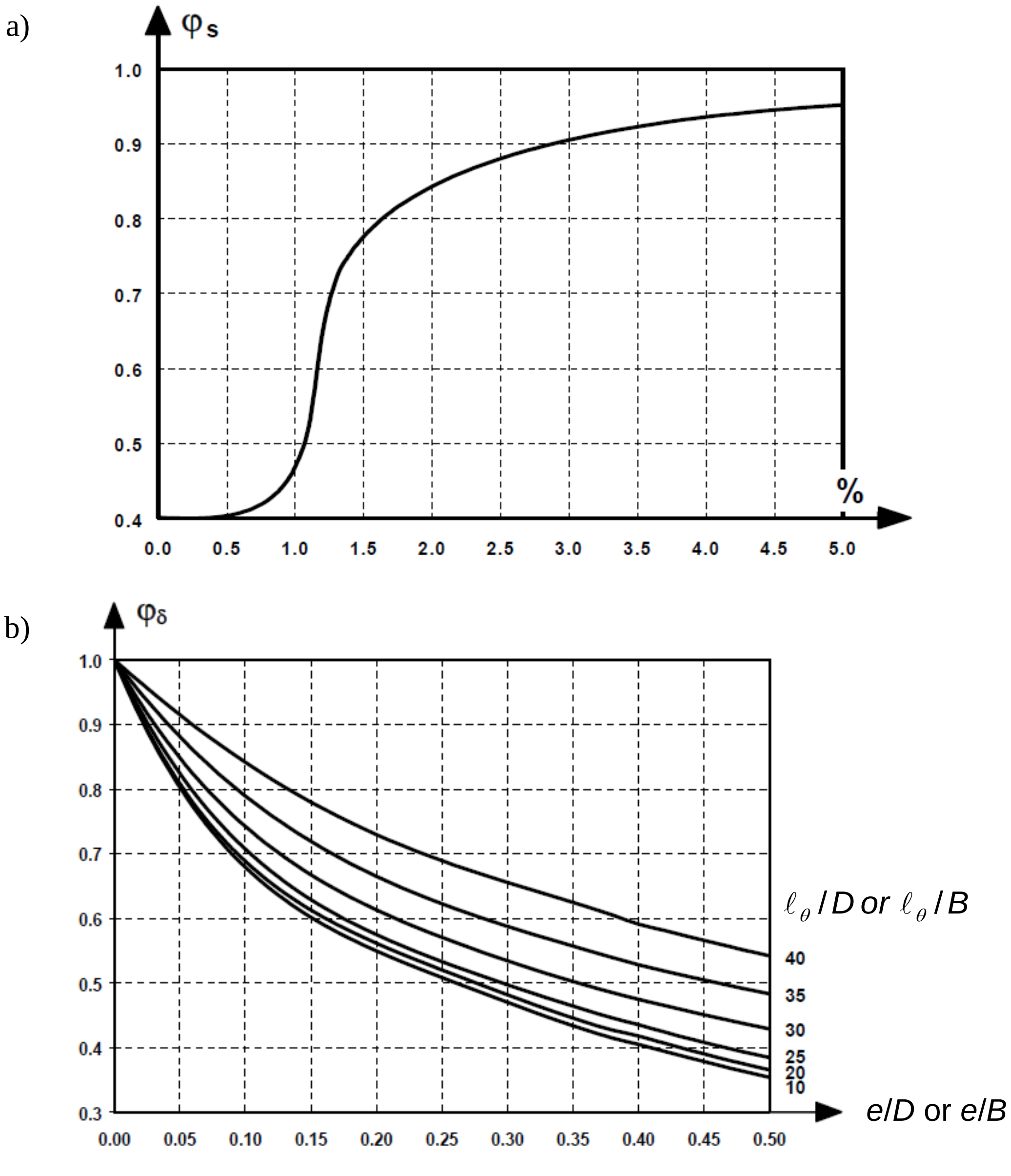

Fig. 9. Correction coefficients from Section H.4 in Annex H [30]: a) Coefficient depending on the percentage of reinforcement; b) Coefficient depending on the eccentricity

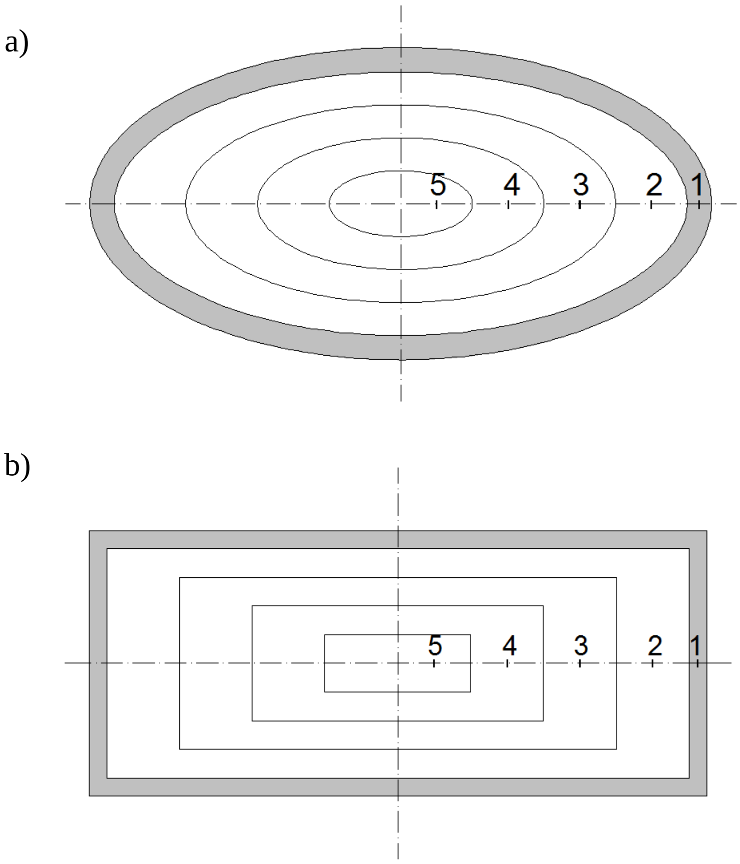

Fig. 10. Discretization of the section for application of EC4 simple calculation model: a) elliptical columns; b) rectangular columns

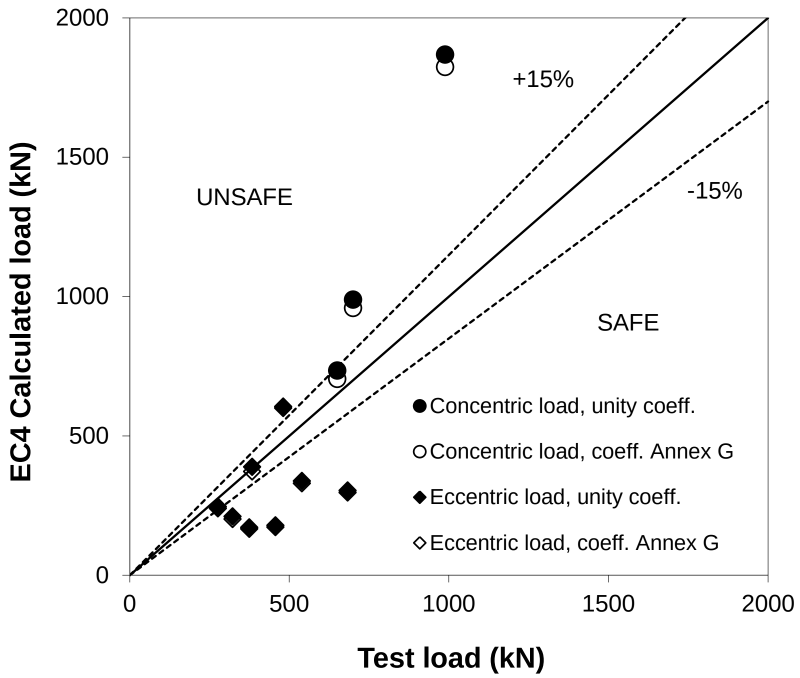

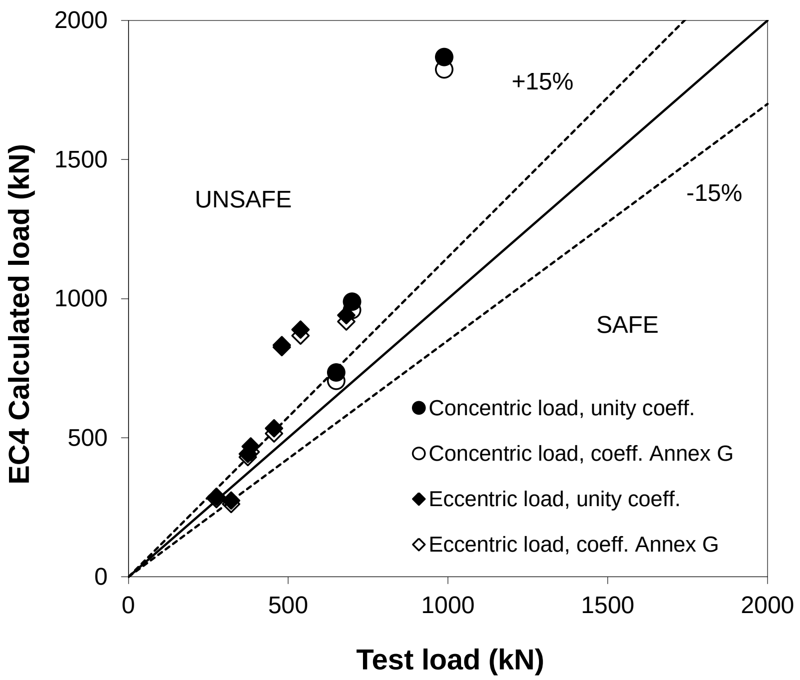

Fig. 11. Comparison between EC4 calculated buckling load and test load, rectangular columns: a) Correction from section H.4 in Annex H, b) Correction from section G.7 in Annex G

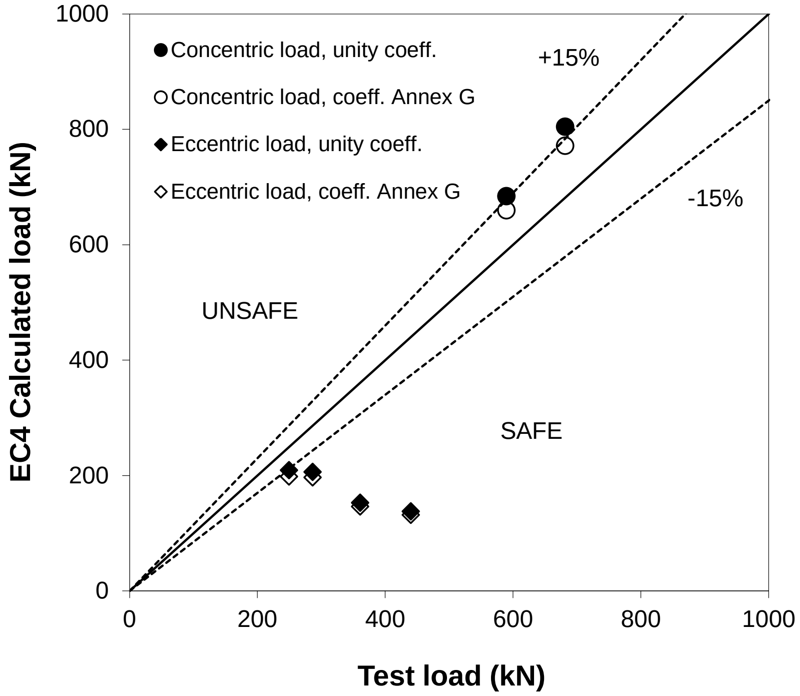

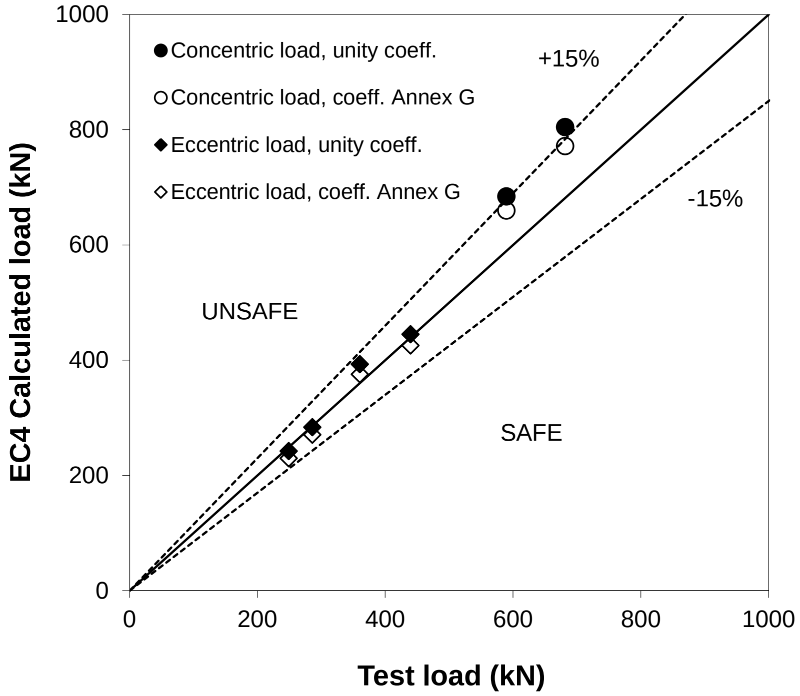

Fig. 12. Comparison between EC4 calculated buckling load and test load, elliptical columns: a) Correction from section H.4 in Annex H, b) Correction from section G.7 in Annex G

Table 1. Test properties and results, rectangular columns

No.	*H* (mm)	*B* (mm)	*t* (mm)	Reinf.	ρ (%)	B.C.	f_c (MPa)	f_y (MPa)	f_s (MPa)	$\bar{\lambda}_y$	$\bar{\lambda}_z$	*e*/*H*	*e*/*B*	Load (kN)	Time (min)
R1	250	150	10	-	0	P-P	37.9	428.3	-	0.53	0.82	0	0	650.8	19
R2	250	150	10	4ϕ16	2.69	P-P	39.6	428.3	527	0.54	0.85	0	0	699.8	23
R3	250	150	10	-	0	P-P	32.0	428.3	-	0.52	0.80	0	0.2	374.7	23
R4	250	150	10	4ϕ16	2.69	P-P	36.3	457.7	527	0.55	0.86	0	0.5	276.9	27
R5	250	150	10	-	0	P-P	36.5	457.7	-	0.54	0.83	0.2	0	456.7	24
R6	250	150	10	4ϕ16	2.69	P-P	32.9	457.7	527	0.54	0.85	0.5	0	322.1	34
R7	350	150	10	-	0	P-P	42. 5	474.0	-	0.41	0.83	0	0	928.9	30*
R8	350	150	10	4ϕ16+4ϕ10	2.61	P-P	38.2	474.0	527 (ϕ16) 575 (ϕ10)	0.40	0.86	0	0	988.8	21
R9	350	150	10	-	0	P-P	37.6	383.3	-	0.38	0.77	0	0.2	540.1	22
R10	350	150	10	4ϕ16+4ϕ10	2.61	P-P	37.3	474.0	527 (ϕ16) 575 (ϕ10)	0.40	0.86	0	0.5	383.9	25
R11	350	150	10	-	0	P-P	38.0	383.3	-	0.38	0.77	0.2	0	683.0	22
R12	350	150	10	4ϕ16+4ϕ10	2.61	P-P	39.7	383.3	527 (ϕ16) 575 (ϕ10)	0.38	0.81	0.5	0	481.4	18*

*Anomalous test

Table 2. Test properties and results, elliptical columns

No.	*H* (mm)	*B* (mm)	*t* (mm)	Reinf.	ρ (%)	B.C.	f_c (MPa)	f_y (MPa)	f_s (MPa)	$\bar{\lambda}_y$	$\bar{\lambda}_z$	*e*/*H*	*e*/*B*	Load (kN)	Time (min)
E7	320	160	12.5	-	0	P-P	37.3	516.4	-	0.52	0.93	0	0	589.8	30
E8	320	160	12.5	4ϕ16	2.57	P-P	41.2	516.4	527	0.54	0.97	0	0	681.9	31
E9	320	160	12.5	-	0	P-P	43.7	516.4	-	0.53	0.94	0	0.2	361.0	30
E10	320	160	12.5	4ϕ16	2.57	P-P	42.4	522.6	527	0.54	0.97	0	0.5	249.4	37
E11	320	160	12.5	-	0	P-P	36.5	522.6	-	0.52	0.93	0.2	0	440.4	32
E12	320	160	12.5	4ϕ16	2.57	P-P	35.5	522.6	527	0.53	0.96	0.5	0	286.5	38

Table 3. Comparison with EC4, rectangular columns

a) Concentrically loaded columns

		Coeff. $\varphi_{i,\theta}$ unity		**Coeff. $\varphi_{i,\theta}$ Annex G**	
	***N* (kN)**	**$N_{fi,Rd}$ (kN)**	**$N/N_{fi,Rd}$**	**$N_{fi,Rd}$ (kN)**	**$N/N_{fi,Rd}$**
R1	650.8	734.38	0.89	704.07	0.92
R2	699.8	989.34	0.71	959.31	0.73
R7	928.9	2047.34	0.45	2012.56	0.46
R8	988.8	1867.87	0.53	1823.59	0.54
		Mean	0.64	Mean	0.66
		Std. dev.	0.19	Std. dev.	0.21

b) Eccentrically loaded columns

		Correction from Section H.4				**Correction from Section G.7**			
		Coeff. $\varphi_{i,\theta}$ unity		**Coeff. $\varphi_{i,\theta}$ Annex G**		**Coeff. $\varphi_{i,\theta}$ unity**		**Coeff. $\varphi_{i,\theta}$ Annex G**	
	***N* (kN)**	**$N_{fi,Rd}$ (kN)**	**$N/N_{fi,Rd}$**	**$N_{fi,Rd}$ (kN)**	**$N/N_{fi,Rd}$**	**$N_{fi,Rd}$ (kN)**	**$N/N_{fi,Rd}$**	**$N_{fi,Rd}$ (kN)**	**$N/N_{fi,Rd}$**
R3	374.7	170.01	2.20	165.69	2.26	441.03	0.85	429.81	0.87
R4	276.9	245.33	1.13	238.29	1.16	287.28	0.96	279.04	0.99
R5	456.7	178.01	2.57	171.96	2.66	533.20	0.86	515.07	0.89
R6	322.1	210.14	1.53	200.63	1.61	274.17	1.17	261.76	1.23
R9	540.1	336.52	1.60	328.41	1.64	888.46	0.61	867.06	0.62
R10	383.9	387.53	0.99	371.36	1.03	468.42	0.82	448.87	0.86
R11	683	302.99	2.25	295.59	2.31	940.51	0.73	917.53	0.74
R12	481.4	603.44	0.80	598.35	0.80	832.55	0.58	825.53	0.58
		Mean	1.63	Mean	1.68	Mean	0.82	Mean	0.85
		Std. dev.	0.65	Std. dev.	0.67	Std. dev.	0.19	Std. dev.	0.21

Table 4. Comparison with EC4, elliptical columns

a) Concentrically loaded columns

		Coeff. $\varphi_{i,\theta}$ unity		**Coeff. $\varphi_{i,\theta}$ Annex G**	
	N (kN)	**$N_{fi,Rd}$ (kN)**	**$N/N_{fi,Rd}$**	**$N_{fi,Rd}$ (kN)**	**$N/N_{fi,Rd}$**
E7	589.8	683.68	0.86	659.42	0.89
E8	681.9	804.12	0.85	771.52	0.88
		Mean	0.86	Mean	0.89
		Std. dev.	0.01	Std. dev.	0.01

b) Eccentrically loaded columns

		Correction from Section H.4				**Correction from Section G.7**			
		Coeff. $\varphi_{i,\theta}$ unity		**Coeff. $\varphi_{i,\theta}$ Annex G**		**Coeff. $\varphi_{i,\theta}$ unity**		**Coeff. $\varphi_{i,\theta}$ Annex G**	
	N (kN)	**$N_{fi,Rd}$ (kN)**	**$N/N_{fi,Rd}$**	**$N_{fi,Rd}$ (kN)**	**$N/N_{fi,Rd}$**	**$N_{fi,Rd}$ (kN)**	**$N/N_{fi,Rd}$**	**$N_{fi,Rd}$ (kN)**	**$N/N_{fi,Rd}$**
E9	361.0	152.72	2.36	146.06	2.47	392.63	0.92	375.50	0.96
E10	249.4	208.91	1.19	198.28	1.26	242.06	1.03	229.74	1.09
E11	440.4	137.79	3.20	131.70	3.34	444.93	0.99	425.27	1.04
E12	286.5	205.92	1.39	196.34	1.46	283.51	1.01	270.32	1.06
		Mean	2.04	Mean	2.13	Mean	0.99	Mean	1.04
		Std. dev.	0.93	Std. dev.	0.97	Std. dev.	0.05	Std. dev.	0.05

LIST OF FIGURE CAPTIONS

Fig. 1. Cross-sectional dimensions and reinforcement arrangement of the tested columns

Fig. 2. Test setup and details of the column ends

Fig. 3. Thermocouple locations: a) elliptical columns; b) rectangular columns

Fig. 4. Evolution of temperatures at mid-height section (A-A'), for column E10.

Fig. 5. View of tested columns after failure: a) column E12 (e/H = 0.5); b) column R11 (e/H = 0.2)

Fig. 6. Results of the fire tests on rectangular columns: a) RHS 250×150×10 mm; b) RHS 350×150×10 mm

Fig. 7. Results of the fire tests on elliptical columns: EHS 320×160×12.5 mm

Fig. 8. Comparison between rectangular and elliptical columns: a) Steel area; b) Fire resistance time; c) Applied load; d) Member slenderness

Fig. 9. Correction coefficients from Section H.4 in Annex H [30]: a) Coefficient depending on the percentage of reinforcement; b) Coefficient depending on the eccentricity

Fig. 10. Discretization of the section for application of EC4 simple calculation model: a) elliptical columns; b) rectangular columns

Fig. 11. Comparison between EC4 calculated buckling load and test load, rectangular columns: a) Correction from section H.4 in Annex H, b) Correction from section G.7 in Annex G

Fig. 12. Comparison between EC4 calculated buckling load and test load, elliptical columns: a) Correction from section H.4 in Annex H, b) Correction from section G.7 in Annex G

LIST OF TABLE CAPTIONS

Table 1. Test properties and results, rectangular columns

Table 2. Test properties and results, elliptical columns

Table 3. Comparison with EC4, rectangular columns

Table 4. Comparison with EC4, elliptical columns